Fluorescence decay kinetics in monodisperse confinements with exchange of probes and quenchers

ARTICLE *in* THE JOURNAL OF PHYSICAL CHEMISTRY · AUGUST 1986

Impact Factor: 2.78 · DOI: 10.1021/j100409a043

3 AUTHORS, INCLUDING:

Mats Almgren
Uppsala University
213 PUBLICATIONS **9,732** CITATIONS
SEE PROFILE

Jan van Stam
Karlstads universitet
68 PUBLICATIONS **1,475** CITATIONS
SEE PROFILE

Fluorescence Decay Kinetics in Monodisperse Confinements with Exchange of Probes and Quenchers

Mats Almgren,*† Jan-Erik Löfroth,‡ and Jan van Stam†

The Institute of Physical Chemistry, University of Uppsala, S-751 21 Uppsala, Sweden, and Department of Physical Chemistry, Chalmers University of Technology and University of Göteborg, S-412 96 Göteborg, Sweden *(Received: October 21, 1985; In Final Form: April 1, 1986)*

The fluorescence decay kinetics of excited probes confined with quenchers in micelles or other approximately monodisperse cells is considered under conditions when both probe and quencher may be exchanged during the lifetime of the excited probe. The exchange may occur either by migration or in processes where two cells make contact and exchange their contents. It is shown that the decay follows, as a good first approximation, an equation of the Infelta type (Infelta, P. P.; Grätzel, M.; Thomas, J. K. *J. Phys. Chem.* **1974**, *78*, 190) but with a generalized interpretation of the parameters. From measurements of the fluorescence decay information on cell size, quenching rate in the cell, and rate of the exchange process may be obtained. The use of the method is illustrated by some results from measurements on the reversed micellar, or microemulsion, phase in the system Triton X-100–toluene–water.

Introduction

Infelta et al.[1] proposed the following equation for the fluorescence decay $F(t)$ of an excited probe, P*, stationary in a micelle and subject to quenching by a migrating quencher, Q:

$$F(t) = A_1 \exp(-A_2 t + A_3(\exp(-A_4 t) - 1)) \quad (1)$$

where $A_1 = F(0)$, assuming δ-pulse excitation at $t = 0$, and

$$A_2 = k_0 + k_q k_- n(k_q + k_-)^{-1}$$

$$A_3 = k_q^2 n(k_q + k_-)^{-2}$$

$$A_4 = k_q + k_-$$

n is the mean number of quenchers in a micelle; k_0 is the fluorescence decay rate constant in the absence of quenchers; xk_q and xk_- are the quenching frequency and the quencher escape frequency, respectively, in a micelle with x quenchers. Tachiya[2] showed that eq 1 follows if, as assumed, the quenching rate constant and quencher escape constant are both proportional to the number of quenchers in the micelle and independent of the number of probes, and the entrance rate of quenchers is independent of the number of quenchers and probes in the micelle. These assumptions require, in effect, that the micelles are of uniform size, and this implies a Poissonian distribution of the quenchers on the micelles.[2] Equation 1 has been used widely for quenching in micellar systems as a basis for methods to determine the micelle size.

A similar confinement of probes and quenchers to small cells is encountered in many microheterogeneous systems. Quite often, however, both probe and quencher may change host cell during the lifetime of the excited probe, and the exchange mechanism may be different from that implied in eq 1. In some microemulsions and reversed micellar phases small water droplets are present, exchanging their contents by fusion–fission processes, i.e. they collide and fuse to a large droplet which again divides into two separate drops.[3,4] Such processes may also occur in normal micelle solutions at high concentrations.[5] If the fused droplets are short-lived the size distribution may remain narrow.

The general appearance of the fluorescence decay in such systems is similar to that given by eq 1: a rapid initial decay followed by a final exponential decay phase. It will be shown in the present contribution that the fluorescence decay in this more general case may be described to a good approximation by an equation of the form of eq 1. Generalized expressions for parameters A_2, A_3, and A_4 will also be presented.

The disposition of the presentation is as follows. The excitation process will select a subset of cells, B, from the totality of cells, M. The number of B cells is assumed small so that no cell contains more than one excited probe. The fluorescence decay will then monitor the transition of B cells into M cells. The various exchange processes result in transitions within the B set, from a B_x cell with x quenchers to a B_y cells with y quenchers. The rules and rates of these transitions will be considered first.

The rate equations for the rate of change of the concentrations of B_x cells are then presented. For simplicity the concentrations will be denoted B_x, B, M_x, and M. From these we derive equations for the rate of change of B and $\langle x \rangle$, the average number of quenchers in the B cells. Consideration of the time evolution of $\langle x \rangle$ leads to the formulation of an approximation that yields analytical solutions for the time dependence of both $\langle x \rangle$ and B.

The time evolutions of $\langle x \rangle$ and B suggest that a stationary state evolves at long times. $\langle x \rangle$ is then constant, $\langle x \rangle_s$, and B decays exponentially. An equation is derived that permits the iterative calculation of the distribution, $b_{x,s} = B_{x,s}/B$, in the stationary state, and from that the value of the important parameter $\langle x \rangle_s$, which contains all information about the exchange processes. Numerical calculations are used to relate $\langle x \rangle_s$ to values of the rate parameters for different exchange processes, and to n, the average number of quenchers in all cells.

We next turn to a test of the approximate solution for the decay of B by comparing it with the results from some numerical solutions of the system of equations for the rate of change of B_x. Finally, some experimental results are presented and discussed briefly as an illustration of the use of the method.

Exchange Mechanisms

We consider a solution of small monodisperse cells in which probes and quenchers are confined. The quenchers are assumed to be randomly distributed over the cells so that

$$M_x = MP(x;n) = Mn^x e^{-n}/x! \quad (2)$$

where $P(x;n)$ is the Poisson distribution and n the average number of quenchers per cell. We assume no explicit limit to the number

† The Institute of Physical Chemistry, University of Uppsala.
‡ Department of Physical Chemistry, Chalmers University of Technology and University of Göteborg.

(1) Infelta, P. P.; Grätzel, M.; Thomas, J. K. *J. Phys. Chem.* **1974**, *78*, 190.
(2) Tachiya, M. *Chem. Phys. Lett.* **1975**, *33*, 289.
(3) Eicke, H. F.; Shepherd, J. C. W.; Steinemann, A. *J. Colloid Interface Sci.* **1982**, *90*, 92.
(4) (a) Fletcher, P. D. I.; Robinson, B. H. *Ber. Bunsenges. Phys. Chem.* **1981**, *85*, 863. (b) Fletcher, P. D. I.; Robinson, B. H.; Bermejo-Barrera, F.; Oakenful, D. G. In *Microemulsions*, Robb, I. D., Ed.; Plenum: New York, 1982; p 221.
(5) Kahlweit, M. *J. Colloid Interface Sci.* **1982**, *990*, 92.

0022-3654/86/2090-4431$01.50/0

of quenchers in a cell but will only consider low values of n, and in practice, therefore, also of x.

The deactivation of the excited probes in the B cells is regarded as a transition from B to M

$$B_x \xrightarrow{k_0+xk_q} M_x \qquad x = 0, 1, \ldots \tag{3}$$

where the rate constants have the same significance as in eq 1.

In the various possible exchange processes the excited probe is conserved. The exchange results in a transition within the B subset

$$B_x \xrightarrow{kw(y;x)} B_y \tag{4}$$

The transition frequency is written as the product of the frequency of transitions from B_x and the conditional probability that they will result in B_y. These factors characterize the three exchange processes that are considered: migration of quencher, migration of excited probe, and exchange in a fusion–fission process.

Migration of quenchers via the intermicellar solution was the case considered by Infelta et al.[1] In their formulation the entrance frequency of quenchers into a micelle was given as the product of a second-order rate constant, k_+, and the concentration, Q_f, of free quencher in the intermicellar solution. This product may be eliminated by the equilibrium condition

$$k_+Q_f = k_-n \tag{5}$$

This has been done in the expressions for parameters A_2 and A_3 of eq 1. The equation, therefore, can be used also in cases when the notion of free quencher is ambiguous, as in a system composed of close-packed cells. The exit frequency of a quencher from a cell with x quenchers is still xk_-, and the average entrance frequency into one cell from all of its neighbors is just nk_-. The case of quenching by multivalent metal ions in SDS was treated in this way recently.[6]

Transitions from B_x occur by both the uptake and the release of a quencher, at a total frequency of $k_-(x + n)$. B_{x-1} is obtained with probability $x/(x + n)$ and B_{x+1} with probability $n/(x + n)$. The transition frequency B_x to B_y can thus be written

$$k_-(x + n)w_q(y;x) = k_-(x\delta_{y,x-1} + n\delta_{y,x+1}) \tag{6}$$

where the Kronecker δ symbol has been used.

The *migration of the excited probe* occurs physically in a similar way but results in quite different transitions. The exit frequency, k_-^P, is assumed independent of the number of quenchers and is thus the same for all B_x. The concentration of free excited probes is assumed negligible, so that also changes in that concentration can be neglected. For any excited probe that leaves a B cell there will thus be another one that enters a M cell. The probability that the new B cell contains y quenchers is $P(y;n)$. The transition frequency is thus

$$k_-^Pw_p(y;x) = k_-^PP(y;n) \tag{7}$$

Finally, we consider the *fusion–fission process*, by which we understand any process in which the contents of two cells is completely mixed. After the process the probes and quenchers are distributed between the two cells at random. This is an idealization of a real "sticky collision" or fusion–fission process—it may be imagined that such processes occur covering the whole scale from complete randomization to exchange of only one probe or quencher. The last extreme case is covered by the transition frequencies of eq 6 and 7.

The frequency of the process will be denoted k_t. In the case that a dilute solution of cells is considered k_t factors into a second-order rate constant and the cell concentration. If, however, we are concerned with close-packed cells the frequency k_t may instead be visualized as a frequency for the formation of holes or channels in the cell walls.

A fusion–fission between B_x and M_m yields B_y with probability

$$w_t(y;x,m) = \frac{(x + m)!}{2^{x+m}y!(x + m - y)!} = \binom{x + m}{y} 2^{-(x+m)} \tag{8}$$

where m must be positive and at least equal to $y - x$. The total probability for a transition of B_x to B_y is obtained by summing over all possible m values, weighing the terms by the Poissonian probability for the M cell to contain m quenchers.

$$w_f(y;x) = \sum_{\substack{m=y-x \\ m>=0}}^{\infty} \binom{x + m}{y} P(m;n)2^{-(x+m)} \tag{9}$$

The transition matrix may easily be evaluated numerically for a given n.

The transition probabilities must be normalized according to

$$1 = \sum_{y=0}^{\infty} w(y;x) \tag{10}$$

It is easily verified that this holds in all three cases. In the following we will need the summations

$$\sum_{y=0}^{\infty} yw_q(y;x) = x + (n - x)/(n + x) \tag{11a}$$

$$\sum_{y=0}^{\infty} yw_p(y;x) = n \tag{11b}$$

$$\sum_{y=0}^{\infty} yw_f(y;x) = (x + n)/2 \tag{11c}$$

Equation 11c is derived in the Appendix.

The Rate Equations

The fundamental equations for the time evolution of the B_x cells are

$$dB_x/dt = -(k_0 + xk_q)B_x - \sum_{y=0}^{\infty} kw(y;x)B_x + \sum_{y=0}^{\infty} kw(x;y)B_y \qquad x = 0, 1, \ldots \tag{12}$$

where

$$kw(y;x) = k_-(x + n)w_q(y;x) + k_-^Pw_p(y;x) + k_tw_f(y;x)$$

The observed fluorescence signal is proportional to the total number or excited probes. Summing all eq 12 we obtain

$$dB/dt = -k_0B - k_q\sum_{x=0}^{\infty} xB_x = -(k_0 + k_q\langle x\rangle)B \tag{13}$$

This decay is exponential if and only if $\langle x\rangle$, the average number of quenchers in B cells, is constant. If the decay has an exponential tail then $\langle x\rangle$ has reached a stationary value $\langle x\rangle_s$. The time evolution of $\langle x\rangle$ from its initial value $\langle x\rangle = n$ to this stationary state is governed by a differential equation which is obtained by adding all eq 12 multiplied by x

$$d\sum_{x=0}^{\infty} xB_x/dt = -k_0\langle x\rangle B - \langle x^2\rangle k_qB - \sum_{x=0}^{\infty}\sum_{y=0}^{\infty}(xkw(y;x)B_x - xkw(x;y)B_y) \tag{14}$$

We have also

$$d\sum_{x=0}^{\infty} xB_x/dt = \langle x\rangle\, dB/dt + B\, d\langle x\rangle/dt \tag{15}$$

Evaluating the double sums with help from eq 10 and 11, and using eq 13 and 15, we obtain from eq 14

$$d\langle x\rangle/dt = -(\langle x^2\rangle - \langle x\rangle^2)k_q + (k_- + k_-^P + k_t/2)(n - \langle x\rangle) \tag{16}$$

The term in the first parentheses of the right hand member is simply the variance, σ_x^2, of the distribution $b_{x,s} = B_{x,s}/B$. Since the variance is always positive and $(n - \langle x\rangle)$ is zero initially, $\langle x\rangle$

(6) Almgren, M.; Linse, P.; Van der Aurewaer, M.; De Schryver, F. C.; Geladé, E.; Croonen, Y. *J. Phys. Chem.* **1984**, *88*, 289.

will decrease from n at a decreasing rate, approaching the stationary state where $d\langle x\rangle/dt = 0$ and $\langle x\rangle = \langle x\rangle_s$.

An Approximate Solution

According to our assumptions the initial distribution b_x is Poissonian. In the case that only the quenchers migrate, it can be shown from Tachiya's treatment[2] that b_x remains Poissonian at all times and thus $\sigma_x^2 = \langle x\rangle$. This is not the case for other exchange mechanisms, however. As a reasonable first approximation we assume that the variance is linearly related to the average

$$\sigma_x^2 = \langle x^2\rangle - \langle x\rangle^2 = \alpha\langle x\rangle + \beta \tag{17}$$

The solution to eq 16 is then

$$\langle x\rangle = (n - \langle x\rangle_s)\exp(-A_4 t) + \langle x\rangle_s \tag{18}$$

where

$$A_4 = \alpha k_q + k_- + k_-^P + k_t/2$$

α and β are fixed by the initial condition

$$n = \alpha n + \beta \tag{19}$$

and by the steady-state condition from eq 16 and 17

$$k_q(\alpha\langle x\rangle_s + \beta) = (k_- + k_-^P + k_t/2)(n - \langle x\rangle_s) \tag{20}$$

With eq 18 the solution to eq 13 is

$$B/B_0 = \exp(-A_2 t + A_3(\exp(-A_4 t) - 1)) \tag{21}$$

with

$$A_2 = k_q\langle x\rangle_s + k_0 \tag{22}$$

$$A_3 = n(1 - \langle x\rangle_s/n)^2 \tag{23}$$

$$A_4 = k_q/(1 - \langle x\rangle_s/n) \tag{24}$$

Equation 21 is in the same form as eq 1; in the Infelta case ($\alpha = 1$, $\beta = 0$, $k_t = k_-^P = 0$) we have from eq 20

$$\langle x\rangle_s/n = k_-/(k_q + k_-) \tag{25}$$

and the parameters A_2, A_3, and A_4 reduces to the expressions given after eq 1. In other cases the relationship between $\langle x\rangle_s/n$ and the rate parameters can be obtained numerically.

The approximate solutions (18) and (21) will be compared in the following with the results from numerical solutions of the equation system (12).

The Stationary State

Even if it is not always possible to observe it experimentally from the fluorescence decay, a stationary state is likely to evolve at sufficiently long times. The distribution of quenchers over cells that still contain excited states is then given by

$$b_{x,s} = B_{x,s}/B \tag{26}$$

All $B_{x,s}$ are deactivated concertedly

$$dB_{x,s}/dt = b_{x,s}\, dB/dt \tag{27}$$

Using this equation and eq 12 and 13 we obtained an equation for the iterative calculation of the stationary distribution

$$b_{x,s} = \frac{\sum_{y=0}^{\infty} kw(x;y)b_{y,s} + k_q\langle x\rangle_s b_{x,s}}{xk_q + k_t + (n + x)k_- + k_-^P} \tag{28}$$

where

$$\sum_{y=0}^{\infty} kw(x;y)b_{y,s} =$$

$$k_t\sum_{y=0}^{\infty} w_f(x;y)b_{y,s} + k_-^P P(x;n) + (x + 1)k_- b_{x+1,s} + nk_- b_{x-1,s} \tag{29}$$

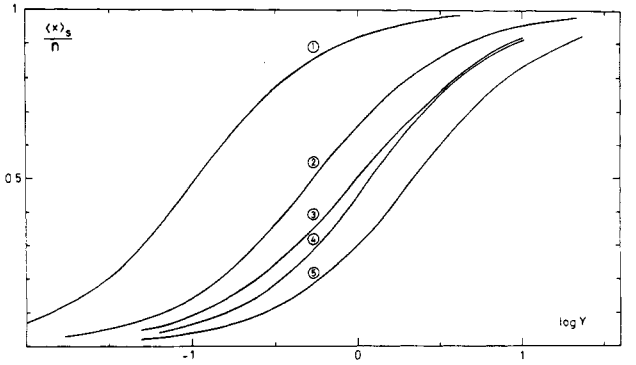

Figure 1. The stationary state ratio of the mean number of quenchers in cells with excited probes and the mean number of quenchers over all cells as a function of the ratio of the pertinent rate constants for different exchange models. (1) Probe migrates ten times faster than quencher $y = k_-/k_q$. (2) Probe and quencher have the same migration rate, y as in 1. (3) Quencher migrates 100 times faster than probe, y as in 1. (4) Probe migrates 100 times faster than quencher, $y = k_-^P/k_q$. (5) Fusion–fission model, $y = k_t/k_q$. All values are for $n = 1$.

The iterative calculation is started by inserting a first approximation for $b_{x,s}$, for instance a Poissonian distribution, in the right-hand member of eq 28. The resulting new set of $b_{x,s}$ values is renormalized by the condition

$$1 = \sum_{x=0}^{\infty} b_{x,s} \tag{30}$$

and $\langle x\rangle_s$ calculated from

$$\langle x\rangle_s = \sum_{x=0}^{\infty} x b_{x,s} \tag{31}$$

The resulting values are again inserted in eq 28 for a new iteration, etc.

Numerical Results

The steady-state distributions were calculated for several models with exchange by fusion–fission or migration at various parameter settings. In Figure 1 values of $\langle x\rangle_s/n$ at $n = 1$ are presented for several models, as a function of k_-/k_q, k_-^P, or k_t/k_q. The curves for the different models are similar, but with important differences. A given value of $\langle x\rangle_s/n$ corresponds to a much higher value of k_t/k_q in the fusion fission model than to k_-/k_q or k_-^P in the migration models. This does not imply, however, that the fusion–fission process is less effective in mixing the contents of the cells than the migration processes; it is only an effect of how k_- and k_t are defined. The difference is clearly seen in the limiting behavior when k_q is much larger than either constant. When the quenching is very rapid $\langle x\rangle_s$ is small, and almost all surviving excited probes are found in B_0 cells, without quenchers. In the fusion–fission model all collisions except those which give no change, i.e. $w(0;0)$, will lead to rapid quenching. In the stationary situation, therefore

$$k_q\langle x\rangle_s \approx k_t(1 - w(0;0)) = k_t(1 - \exp(-n/2)) \tag{32}$$

This can be compared with the case when only quenchers migrate.

$$k_q\langle x\rangle_s = k_- k_q(k_- + k_q)^{-1} n \approx k_- n \tag{33}$$

Thus, the same value of $\langle x\rangle_s$ is obtained in the two processes if

$$k_-/k_q = k_t(1 - \exp(-n/2))/(k_q n)$$

which, at $n = 1$, yields $k_-/k_q = 0.393 k_t/k_q$.

It should also be noticed that $\langle x\rangle_s/n$ rises faster for the model where both probe and quencher migrate (curve 2 in Figure 1) than when the migration is due mainly to the quencher (curve 3) or to the probe (curve 4). The migration of the quencher gives larger $\langle x\rangle_s/n$ values than migration of the probe, probably because of the possibility for the excited probe to escape to empty micelles.

TABLE I: Stationary Distribution $b_{x,s}$ of Quenchers in Cells with Excited Probes for Some Different Exchange Models (n = 1)

		$k_t = 0$			
	$k^P = k_- = 0$ $k_t/k_q = 2$	$k^P/k_- = 1$ $k_-/k_q = 0.5$	$k^P/k_- = 0.01$ $k_-/k_q = 1$	$k^P/k_- = 100$ $k^P/k_q = 1.11$	$b_{x,s} = P(x;\langle x\rangle_s)$
$b_{0,s}$	0.6309	0.6279	0.6053	0.6453	0.6053
$b_{1,s}$	0.2779	0.2826	0.3037	0.2533	0.3039
$b_{2,s}$	0.0740	0.0724	0.0763	0.0781	0.0763
$b_{3,s}$	0.0145	0.0143	0.0128	0.0188	0.0128
$b_{4,s} \times 10^3$	2.29	2.41	1.63	3.69	1.60
$b_{5,s} \times 10^4$	3.02	3.61	1.67	6.07	1.61
$b_{6,s} \times 10^5$	3.45	4.82	1.46	8.50	1.35
$b_{7,s} \times 10^6$	3.48	5.76	1.15	10.65	.97
$\langle x\rangle_s$	0.4803	0.4820	0.5021	0.4843	0.5021

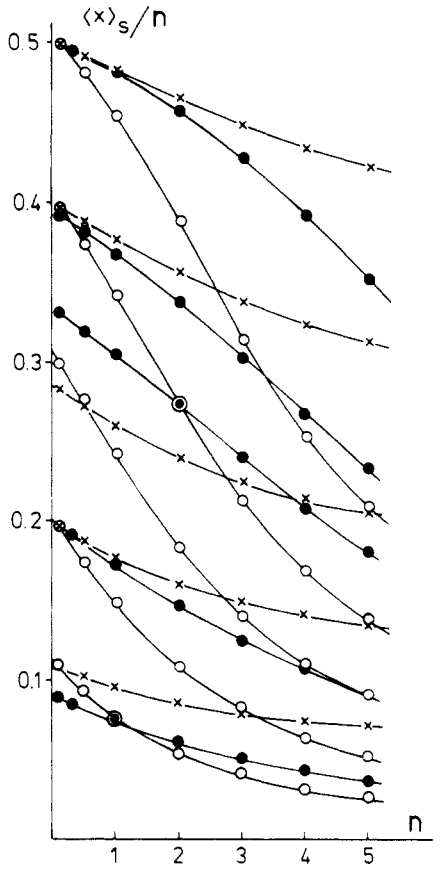

Figure 2. Calculated values of $\langle x\rangle_s/n$ as a function of n for three exchange models: ×, quencher and probe migrate equally fast; ●, fusion–fission model; ○, only probe migrates. The values of k_-/k_q, $k_-{}^P/k_q$, and k_t/k_q were chosen so as to cover a realistic range of values on the y axis.

This point is illustrated by the distributions $b_{x,s}$ presented in Table I, where it also can be noticed that the distribution is Poissonian only in the Infelta case.

When the exchange mechanism is known the calculated plots of $\langle x\rangle_s/n$ provide values of the corresponding rate constant ratios from the experimental estimates of $\langle x\rangle_s$. It is important, therefore, to find a means to discriminate between different exchange mechanisms. The variation of $\langle x\rangle_s/n$ with n (or experimentally, the quencher concentration) would in principle be helpful, as shown in Figure 2. There are appreciable differences between the different models. In the Infelta case there is no variation with n (not shown), whereas $\langle x\rangle_s/n$ decreases in all other cases, most rapidly when only probes are migrating. It remains to be seen how well these changes can be measured experimentally. It should also be remembered that there might be other causes for the observed variation, such as a cell size polydispersity which is known to produce a decrease in the observed average aggregation number with the quencher concentration.[7]

(7) Almgren, M.; Löfroth, J.-E. *J. Chem. Phys.* **1982**, *76*, 2734.

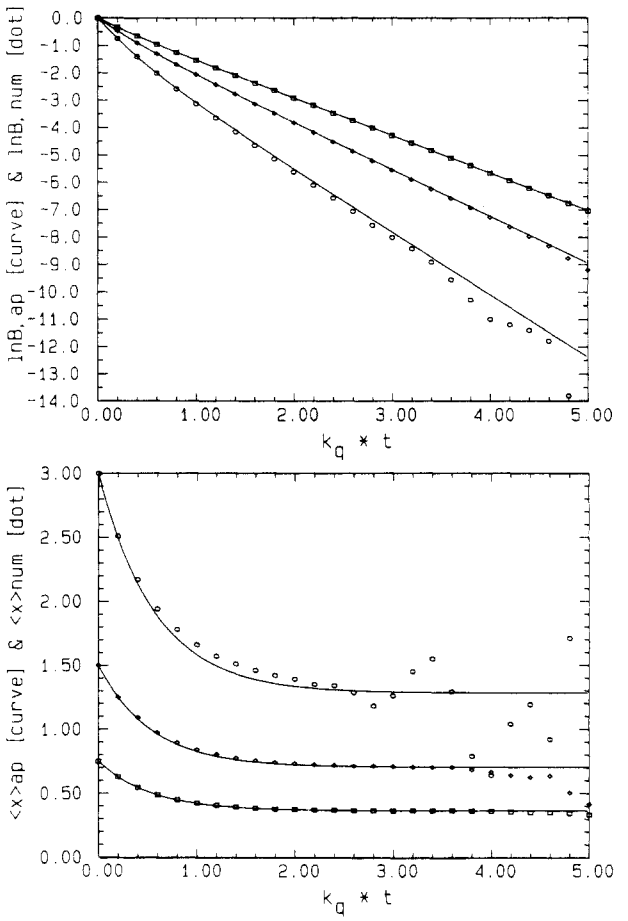

Figure 3. (a, top) Logarithmic decay curve and (b, bottom) decay of $\langle x\rangle$ for the fusion–fission model with $k_t/k_q = 2$, $k_0/k_q = 1$, and $n = 0.75$ (□); 1.50 (◇); 3.0 (○). The full drawn curves represent the approximate solutions according to eq 21 and 18; the dots were obtained from numerical solution of equation system (12).

A Numerical Test of the Approximation

The equation system (12) was solved numerically, using a Runge–Kutta routine, for several examples. It was necessary to continue the integrations down to very low concentrations of components. This caused some numerical problems which were not completely controlled and sometimes resulted in oscillations at long times. The approximate solutions, eq 21 and 18, are compared in Figures 3 and 4 to the numerical results for the decays of ln B and $\langle x\rangle$ in some representative cases. It is apparent that the numerical results (dots) for ln B at long times fall below the approximate solution, although the limiting slope is correct. This is due to the fact that the approximation gives a correct initial solution for the decay, but at intermediate times predicts too low values for $\langle x\rangle$, and thus also too slow a consumption of excited states. Hence, in the final exponential part of the decay where the decay rate is again correct, the approximate solution gives too high a concentration of excited states.

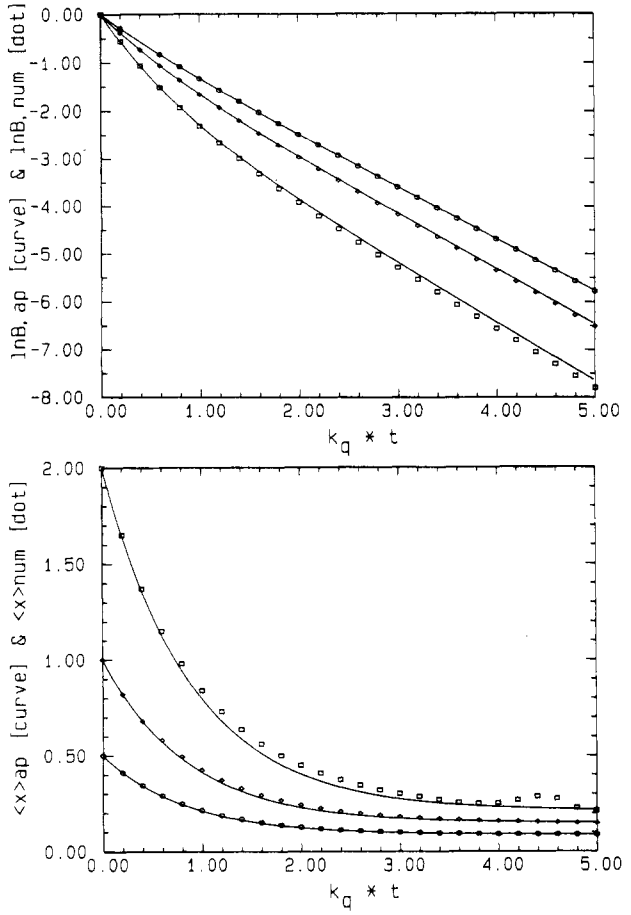

Figure 4. Same as Figure 3 for probe migration models with k_{-P}/k_q = 0.25, k_0/k_q = 1.0, and n = 0.50 (○); 1.0 (◇); 2.0 (□).

The character of the approximate solution as a correct initial solution is demonstrated by prescribing eq 21 as a solution and determining the parameters A_2, A_3, and A_4 as follows.

The limiting values of dB/dt for $t \rightarrow \infty$ from eq 13 and 21 are set equal giving eq 22 for A_2. Comparison of the initial values of dB/dt and d^2B/dt^2 from eq 13 and 21 yields

$$k_0 + k_q n = A_2 + A_3A_4 \quad (34)$$

$$k_0^2 + 2k_0k_qn + k_q^2\langle x^2\rangle_0 = (A_2 + A_3A_4)^2 + A_3A_4^2 \quad (35)$$

Using the fact that $\langle x^2\rangle_0 = \langle n^2\rangle = n^2 + n$ for a Poissonian distribution we retrieve eq 23 and 24 for A_3 and A_4.

Although the deviations in Figures 3 and 4 appear small, they may be important in the delicate fitting procedure that is used in evaluation of experimental data. A simple test was obtained by fitting eq 21 by a nonlinear least-squares method to the values obtained by numerical integration for some test systems. The results are reported in Table II. Some general conclusions are possible. The estimated values are good or very good at low quencher concentrations (low n values), but large errors appear at about n = 2 or greater. This is in particular the case for $\langle x\rangle_s/n$, and makes it difficult to use the variation of this parameter with n for a test of the exchange mechanism.

The conclusion from this preliminary numerical study is that we can have some faith in estimates of n, k_q, and $\langle x\rangle_s$ obtained by fitting the experimental data to the approximate model for low quencher concentrations, but that it is difficult to discriminate between different exchange mechanisms in this way.

An Experimental Test

Measurements on $Ru(bpy)_3^{2+}$ with methylviologen as quencher were performed in the microemulsion phase of the system Triton X-100 (a nonionic surfactant)–toluene–water at several compositions as shown in Figure 5. The results will be discussed here as an illustration of the numerical and experimental problems encountered in practice; the information obtained about the microemulsion is discussed elsewhere.[8]

TABLE II: Estimates of n, $\langle x\rangle_s$, and k_0/k_q from Fitting of the Approximate Equation for ln B vs. t to Values Obtained by Numerical Integration of Equation System (12) for Some Models

numerical model[a]		approximate model		
n	$\langle x\rangle_s/n^b$	n	$\langle x\rangle_s/n$	k_0/k_q
		Probe Migration Model		
		k_{-P}/k_q = 0.25		
0.25	0.186	0.250	0.187	1.000
0.75	0.158	0.747	0.161	1.006
1.50	0.124	1.500	0.124	1.021
2.00	0.106	1.801	0.036	1.163
3.00	0.079	2.705	0.005	1.251
		k_{-P}/k_q = 1.00		
0.25	0.489	0.250	0.490	1.000
0.75	0.464	0.756	0.458	1.005
1.50	0.418	1.506	0.415	1.028
2.00	0.382	1.984	0.389	1.059
3.00	0.306	2.230	0.174	1.671
		Fusion–Fission Model		
		k_t/k_q = 0.300		
0.25	0.125	0.249	0.128	1.000
0.75	0.114	0.753	0.117	1.000
1.50	0.100	1.499	0.100	1.009
2.00	0.0912	1.991	0.0945	1.014
3.00	0.0762	2.980	0.0823	1.030
		k_t/k_q = 2.00		
0.25	0.495	0.253	0.485	1.000
0.75	0.486	0.755	0.484	1.000
1.50	0.469	1.502	0.468	1.010
2.00	0.457	1.994	0.460	1.020
3.00	0.427	2.969	0.441	1.058

[a] k_0/k_q = 1.00 in all cases. [b] $\langle x\rangle_s$ was obtained by iterative solution of eq 28.

The fluorescence decay curves at high toluene and low water content are as expected for quenching in water droplets with some intercommunication, Figure 6. At higher water and high surfactant concentrations the model still works, but now with very pronounced exchange between the droplets. The experimental curves show a well-developed exponential tail following the initial nonexponential phase.

At each composition measurements were performed (as described earlier[9]) without quencher and at five quencher concentrations. No deconvolution was necessary due to the very narrow instrument response on the time scale used with the long-lived $Ru(bpy)_3^{2+}$. All data from one composition were analyzed together in a global analysis,[10] in which the model defined by eq 21–24 was fitted simultaneously to all five data sets obtained with quencher present. In this fitting k_0 was fixed at the value estimated from the measurement without quencher. Also k_q was common for the five data sets, whereas n and $\langle x\rangle_s$ were different for each set. More accurate estimates of n, $\langle x\rangle_s$, and k_q should be obtained in this way than if each data set were analyzed separately. The fit to the model was excellent in all cases, as exemplified in Table III with data belonging to the same compositions as the decay curves in Figure 6.

Figure 7 presents plots of $\langle x\rangle_s/n$ and n/Q vs. n for almost all compositions. In most cases the variation of n/Q is slight—it should be constant according to the model—and regular, usually an increase with n is obtained at high, and a decrease at low water concentration. Some of the solutions show an abnormal behavior both regarding n/Q and $\langle x\rangle_s/n$. It is evidently not possible to discriminate between different exchange mechanisms from such

(8) Almgren, M.; Swarup, S.; Löfroth, J.-E.; van Stam, J. *Langmuir*, in press.

(9) Löfroth, J.-E. Ph.D. Thesis, University of Göteborg, Göteborg, Sweden, 1982.

(10) (a) Knutson, J. R.; Beechem, J.; Brand, L. *Chem. Phys. Lett.* **1983**, *102*, 501. (b) Löfroth, J.-E. *Eur. Biophys. J.* **1985**, *13*, 45. *J. Phys. Chem.* **1986**, *90*, 1160. *Anal. Instrumen. (N.Y.)*, in press.

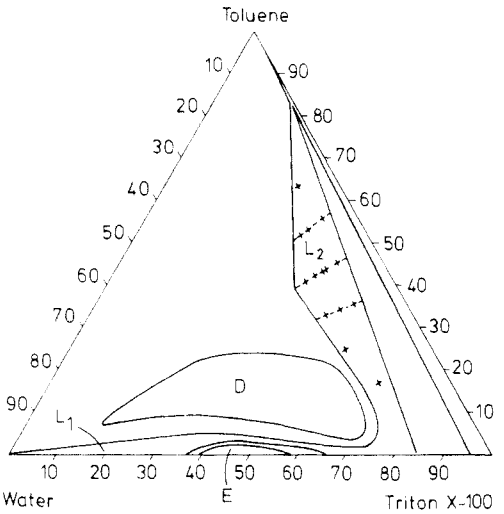

Figure 5. Phase diagram at 22 °C for Triton X-100–toluene–water. L_1 and L_2 are parts of the same one-phase area; normal micelles are found in L_1 and inversed micelles or water droplets in L_2. The compositions of studied solutions are marked ×. D is the lamellar phase and E the hexagonal phase.

TABLE III: Estimated Parameter Values and Goodness-of-Fit Measures from a Global Analysis of Six Decay Curves Pertaining to Different Quencher Concentrations at Each of Two Compositions

$10^3[MV^{2+}]$, mol kg^{-1}	n	$\langle x\rangle_s$	χ_v^{2a}	z^b
	Composition 1[c]			
1.157	0.144 ± 0.014	0.065 ± 0.005	1.08	0.36
2.226	0.307 ± 0.015	0.117 ± 0.006	1.09	0.72
3.518	0.499 ± 0.016	0.187 ± 0.008	1.03	1.08
4.350	0.603 ± 0.016	0.232 ± 0.008	1.14	0.99
6.242	0.900 ± 0.017	0.350 ± 0.010	0.96	0.39
7.597	1.111 ± 0.017	0.436 ± 0.012	0.88	0.52
	Composition 10[d]			
0.648	0.205 ± 0.012	0.013 ± 0.003	1.08	1.74
1.255	0.412 ± 0.013	0.023 ± 0.004	1.05	0.18
1.780	0.571 ± 0.011	0.032 ± 0.003	1.10	0.24
2.401	0.748 ± 0.014	0.040 ± 0.005	1.25	0.14
3.081	0.954 ± 0.015	0.046 ± 0.005	0.97	0.36
3.679	1.115 ± 0.016	0.050 ± 0.005	0.99	1.82

[a] Reduced χ^2 test. [b] Runs test. [c] Composition 1 in Table IV. The probe concentration was 5×10^{-5} M. $\tau_0 = 666 \pm 10$ ns ($\chi_v^2 = 1.13$; $z = 0.03$); $k_q = (5.55 \pm 0.076) \times 10^6$ s^{-1}. [d] Composition 10 in Table IV. Probe concentration 5×10^{-5} M. $\tau_0 = 582 \pm 9$ ns ($\chi_v^2 = 1.06$; $z = 0.40$); $k_q = (5.55 \pm 0.28) \times 10^6$ s^{-1}.

data. For comparison, some curves representing the expected behavior according to the fusion–fission mechanism are also shown in Figure 7.

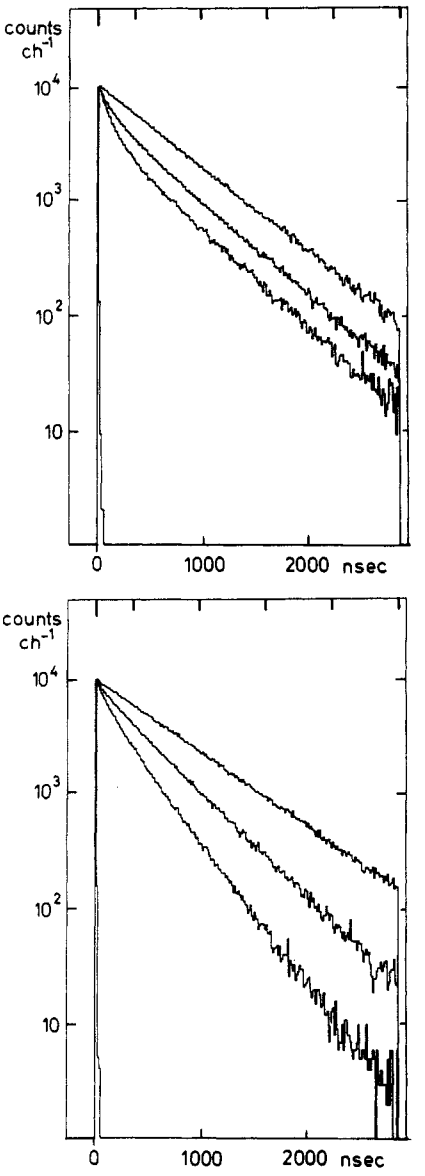

Figure 6. Examples of experimental fluorescence decay curves: (a, top) $T/T_x = 50/50$; water 9.5% w/w; $n = 0$; 0.57; 1.12; $\langle x\rangle_s/n = 0$; 0.057; 0.045; (b, bottom) $T/T_x = 20/80$; water 15.0% w/w; $n = 0$; 0.50; 1.11; $\langle x\rangle_s/n = 0$; 0.38; 0.39. The values of n and $\langle x\rangle_s/n$ were estimated in a global analysis as discussed in the text. As indicated, the instrument response function is appreciable only in the first few channels.

One reason for systematic deviations is, of course, the fact that the model is an approximation, as discussed above. Another

TABLE IV: Droplet Concentration, Number of Water Molecules per Droplet, and Rate Parameters from Fluorescence Quenching Studies of the L-2 Phase of Triton X-100–toluene–Water at 25 °C

no.	composition T/T_x[a]	composition H_2O_x[b]	droplet concn, mmol/kg	N_{H_2O}	$\langle x\rangle_s/n$ at $n = 1$	$10^{-6}k_q$, s^{-1}	$10^{-6}k_t$, s^{-1}	$10^{-9}k_c$, mol^{-1} kg s^{-1}
1	20/80	15.00	7.20	1155	0.39	3.26	5.5	0.75
2	30/70	17.70	3.92	2504	0.47	2.01	4.0	1.0
3	40/60	17.90	2.58	3854	0.42	1.76	2.9	1.1
4	40/60	14.44	3.52	2276	0.195	3.48	1.75	0.50
5	40/60	11.40	4.37	1448	0.125	5.09	1.75	0.40
6	50/50	18.40	1.68	6084	0.34	1.93	2.3	1.35
7	50/50	15.90	2.00	4412	0.28	2.14	1.9	0.95
8	50/50	13.20	2.44	3000	0.123	3.34	1.15	0.45
9	50/50	12.60	2.64	2648	0.080	3.90	0.85	0.32
10	50/50	9.50	3.17	1660	0.048	5.55	0.7	0.22
11	60/40	13.90	1.16	6670	0.190	2.05	1.1	0.95
12	60/40	12.00	1.48	4490	0.125	2.70	0.95	0.63
13	60/40	7.53	1.93	2165	0.026	5.98	0.38	0.20
14	70/30	8.50	0.73	6500	0.18	2.06	1.05	1.45

[a] Weight ratio toluene/Triton X-100. [b] Percent by weight.

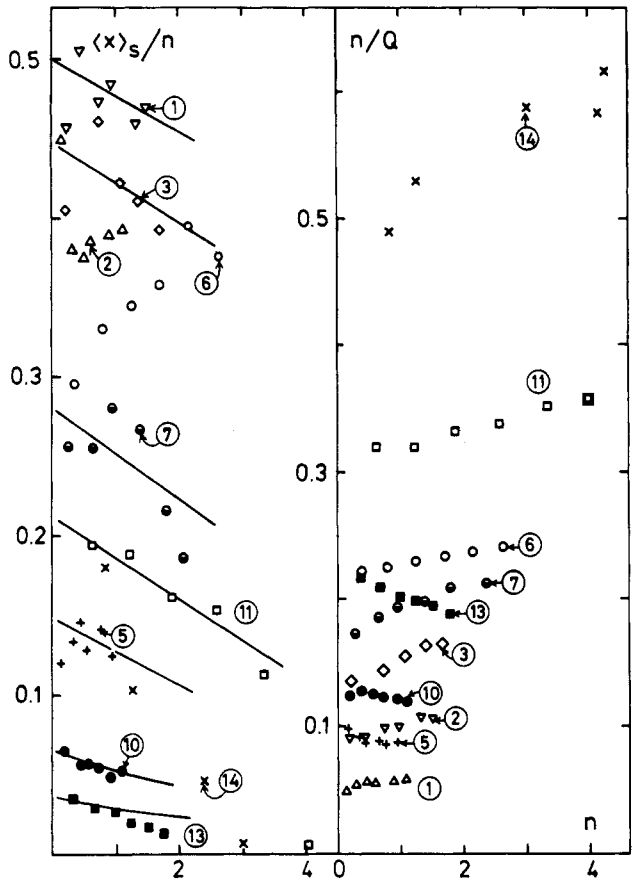

Figure 7. Estimated values of $\langle x\rangle_s/n$ and n/Q as a function of estimated n. The solution compositions are identified with numbers that refer to Table IV.

important factor is that the fitting was restricted to intensities exceeding 100 counts per channel. The length of the time range that can be used depends on the quencher concentration, and it may become too short for a proper determination of the stationary decay at high quencher concentrations in some cases. A third source to systematic errors is the variation of the ionic strength in the water pools with the quencher concentration. There are several possibilities for improvements by a critical design of the experiments and a critical choice of the method for data analysis.

Table IV summarizes the results of the measurements. The mean number of water molecules in the droplets (calculated from the droplet concentration by assuming that all water is in the drops) varies regularly; most evident is the growth with increasing water concentration. The values of k_t/k_q and k_t were obtained from the estimated values of $\langle x\rangle_s/n$ at $n = 1$ and Figure 1, assuming that the exchange occurred by the fusion–fission mechanism. The rate constant k_t is the frequency of collisions resulting in exchange; by division with the droplet concentration a second-order rate constant k_c for successful collisions is obtained which varies appreciably less than k_t itself. k_c is probably somewhat smaller than the diffusion-limited rate constant in all cases, but certainly not by more than a factor of 50. Although the significance of this second-order constant is doubtful in solutions were the colliding entities are very closely spaced, it is evident that not all collisions are successful. Interestingly, Fletcher et al. estimated a corresponding second-order rate constant in the system AOT–heptane–water and concluded that only 10^{-3} of the collisions were successful.[4] The Triton X-100 system seems more similar to soft-core cosurfactant type microemulsions than to the hard-core AOT type.[11,12]

Acknowledgment. This work has been supported by grants from the Swedish Natural Science Research Council.

Appendix

Proof of

$$\sum_{y=0}^{\infty} y w_f(y;x) = (n + x)/2 \tag{11c}$$

$$\sum_{y=0}^{\infty} y w_f(y;x) = \sum_{y=1}^{\infty} y w_f(y;x) =$$

$$\sum_{y-1=0}^{\infty} \sum_{\substack{m=y-x \\ m>=0}}^{\infty} y \binom{m+x}{y} P(m;n)2^{-(m+x)} =$$

$$\sum_{y-1=0}^{\infty} \sum_{\substack{m=y-x \\ m>=0}}^{\infty} (m+x) \binom{m+x-1}{y-1} P(m;n)2^{-(m+x)}$$

We get two double sums, with terms multiplied by m and x, respectively. The first sum can be restricted to terms with $m > 0$

$$\sum_{y-1=0}^{\infty} \sum_{\substack{m=y-x \\ m>0}}^{\infty} m \binom{m+x-1}{y-1} P(m;n)2^{-(m+x)} +$$

$$\sum_{y-1=0}^{\infty} \sum_{\substack{m=y-x \\ m>=0}}^{\infty} x \binom{m+x-1}{y-1} P(m;n)2^{-(m+x)} =$$

$$(n/2) \sum_{y-1=0}^{\infty} \sum_{\substack{m-1=y-1-x \\ m-1>=0}}^{\infty} \binom{m-1+x}{y-1} P(m-1;n)2^{-(m-1+x)} +$$

$$(x/2) \sum_{y-1=0}^{\infty} \sum_{\substack{m=y-x \\ m>=0}}^{\infty} \binom{m+x-1}{y-1} P(m;n)2^{-(m+x-1)} =$$

$$(n/2) \sum_{y-1=0}^{\infty} w_f(y-1;x) + (x/2) \sum_{y-1=0}^{\infty} w_f(y-1;x-1) = (n+x)/2$$

where eq 10 was utilized in the last step.

Registry No. $Ru(bpy)_3^{2+}$, 18955-01-6; methylviologen, 1910-42-5; toluene, 108-88-3; Triton X-100, 9002-93-1.

(11) Lindman, B.; Stilbs, P. In *Surfactants in Solution*, Mittal, K. L., Lindman, B., Ed.; Plenum: New York, 1984; p 1651.
(12) Tadros, Th. F., ref 11, p 1501.